Powder Technology 192 (2009) 384–388

Contents lists available at ScienceDirect

Powder Technology

journal homepage: www.elsevier.com/locate/powtec

Short communication

Shape of a particle curtain falling in stagnant air

Chrestella Wardjiman [a,*], Andrew Lee [b], Madoc Sheehan [b], Martin Rhodes [a]

[a] Department of Chemical Engineering, Monash University, Victoria 3800, Australia
[b] James Cook University, School of Engineering, Townsville, Queensland 4811, Australia

ARTICLE INFO

Article history:
Received 20 April 2008
Received in revised form 7 November 2008
Accepted 9 January 2009
Available online 19 January 2009

Keywords:
Particle curtain
Free fall
Stagnant air

ABSTRACT

The dynamics of a free falling particle curtain were analysed and studied in the laboratory. In the experiments a steady, uniform, high-voidage stream of particles was fed through a rectangular slit to form a curtain across the entire width of a horizontal duct of cross-section of 0.15 × 0.60 m. The thickness of the particle stream at the inlet was varied over the range 2–10 cm by varying the width of the rectangular slit. The particle flow rates were maintained constant at approximately 0.040 kg/s. The shape of the particle curtain was recorded using a high-speed video camera. Our results indicated a low voidage curtain led to diverging curtain; increasing the initial voidage of the particle stream caused the curtain to become less divergent; further increase the voidage of the particle stream caused the curtain to become increasingly convergent. The shape of particle curtain was analysed using an Eulerian–Eulerian computational fluid dynamics (CFD) model. Reasonable agreement was found between the experiments and the CFD model predictions.

© 2009 Elsevier B.V. All rights reserved.

1. Introduction

Many applications of industrial significance involve a stream of free falling particles in quiescent air and the characteristics of such a system have been the subject of interest of many researchers [7,12,13,18]. For example, Wypych et al. [18] found that particles falling in quiescent air could form a relatively coherent diverging powder stream. The authors noticed that the particles within the stream had less interaction with the surrounding air than if they were falling independently. The authors reported that the surrounding air was continuously entrained into the falling stream and the amount of entrained air was directly proportional to the falling height. These observations led them to conclude that the main core of the falling powder was surrounded by a turbulent layer of fine dust, which escaped easily to the surrounding air.

Interestingly, in the studies carried out by Darton [4] on the flow of uniformly-sized solid particles from a circular hole under gravity, the resulting powder jets were observed to converge in some cases. A detailed study was done by Pring et al. [13] where they focused on the free fall of particulate solids at the transfer point where solids drop from one level to another. They argued that a falling curtain of particles is like a low efficiency fan, drawing in air at the top and forcing it out at the bottom where the force exerted by the falling particles creates a negative pressure within and about the edges of the curtain as it falls. The authors further suggested that the differential between the normal pressure outside the curtain and the reduced pressure within the curtain induces a flow of air toward and along with the falling particles. The authors found that the rate of induced air flow was proportional to the falling particle velocity. Hemeon [7] and Plinke et al. [12] later showed that the induced air flow within a falling particle curtain was a major contributing factor to dust generation.

The converging phenomenon was not restricted to falling particles systems. Rothe and Block [14] observed similar converging phenomena when they sprayed a liquid into a gas environment. The authors suggested that the static pressure inside the spray was below the ambient pressure and air entered the spray nearly perpendicular to the drop trajectories and then turned rapidly to the axial direction as it passed into the spray. The authors argued that as the entrained gas entered the spray, it dragged the liquid drops at the outer regions of the spray inward, causing the spray to contract. The author found that the magnitude of the contraction depended on how effectively the spray drops entrained gas and on how strongly the inflowing gas pushed the drops from their original trajectories.

Ogata et al. [11] measured the gas axial velocity profiles of a free-falling particle jet of glass beads with a relatively uniform diameter in quiescent surroundings. The authors suggested that the velocity profile near the orifice was uniform and further from the orifice the velocity took its maximum value at the centerline and decreased away from the centerline in the horizontal direction. Uchiyama [16] simulated the particulate jet generated by particles of uniform size falling from a slit orifice into unbounded quiescent air using a two-dimensional vortex method for gas-particle two-phase free turbulent flows. The author observed that the vertical gas velocity was maximum at centerline, and decreased away from the centerline in the horizontal direction and this maximum velocity increased with falling distance, which agreed with Ogata experimental results.

* Corresponding author.
E-mail address: Chrestella.Wardjiman@college.monash.edu.au (C. Wardjiman).

0032-5910/$ – see front matter © 2009 Elsevier B.V. All rights reserved.
doi:10.1016/j.powtec.2009.01.009

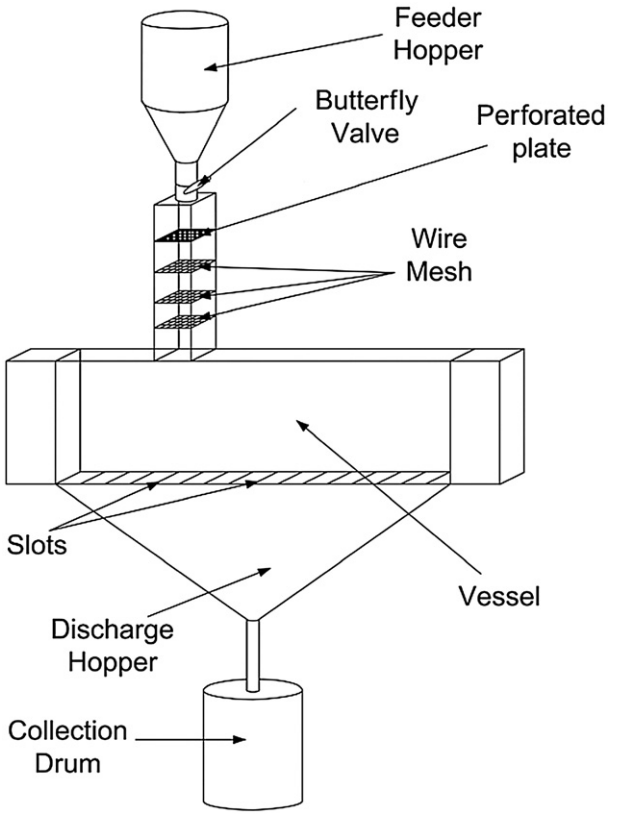

Fig. 1. Schematic diagram of experimental setup.

The aim of this study was to investigate the changing shape of a free falling high-voidage stream of particles with changing initial stream voidage. In the present study, a particle curtain is generated to span across the entire width of the vessel. A computational fluid dynamics (CFD) was used in analysing the shape of particle curtain.

CFD has successfully been used to model a wide range of gas–solid systems, such as fluidized beds (for example Du et al. [5] and Nakamura and Watano [9] and pneumatic conveying (for example Hidayat and Rasmuson [6]). A number of different approaches have been developed for simulating two phase gas–solid systems, for example Eulerian–Eulerian and Eulerian–Lagrangian approaches, each appropriate for a specific set of circumstances. In situations involving large numbers of particles, the Lagrangian methods of tracking individual particles is often prohibitive, thus the Eulerian–Eulerian approach is generally used for large systems [3].

2. Experimental

2.1. Particle curtain apparatus

A schematic of the experimental system was shown in Fig. 1. The apparatus consisted of the following parts: vessel, solid feeder, solid transport system, collection drum, and measurement system. The vessel had inside dimensions of 0.15 m width, 0.60 m height and 2.40 m length. The side walls of the vessel were made of transparent Perspex. At the base of the vessel, there were slots that could be opened or closed. During each experiment, most of the slots were closed, and at specific location where the particle curtain falls, the slots were opened. They were installed to create a smooth wall at the bottom of the vessel. The apparatus was also equipped to study the behaviour of a particle curtain falling through a flowing air stream, though this was not the subject of the present study.

The experiments were performed using silica sand with Sauter mean diameter of 204 μm. The particle density of the silica sand was 2640 kg/m^3. A curtain of particles with steady mass flow rate and uniform particle distribution was created by steadily feeding solids from a hopper through a rectangular duct in which a perforated plate and three pieces of wire mesh were secured. The solids from the feed hopper flow through the perforated plate and each piece of wire mesh in turn for uniform dispersion across the cross-section of the duct. The opening of duct outlet was adjustable so that uniform, steady curtains of variable thickness could be created.

The desired curtain was then established by first installing the appropriate perforated plate to establish the required mass flow rate and then adjusting the feeder outlet dimension in the horizontal direction to obtain the desired curtain thickness. The particles were discharged from the vessel to a collection drum underneath the vessel via a hopper. Solids caught in the collection drum during an experiment were transferred pneumatically to the feed hopper before the start of the next experiment.

2.2. Measurements

The particle curtain was imaged in elevation through the Perspex side wall of the vessel using a digital high-speed camera. The edges of the particle curtain were then tracked frame by frame. Fig. 2 was a typical image of particle curtain showing the tracked edges.

The vertical components of particle velocities along the approximate centreline of particle curtain were obtained by capturing the individual particle images using a digital high speed camera at 1930 frames/s and tracking the particles frame by frame. In order to measure the solid mass flow rate, the collection drum was suspended by a load cell during the experiments. The changes in voltage with time in the load cell were detected and recorded by the data acquisition system for the mass flow rate calculation.

3. CFD model

The falling curtain of solids within the stagnant air was simulated using a steady-state solution to the unsteady–state governing equations for a two-phase system using a Eulerian–Eulerian approach.

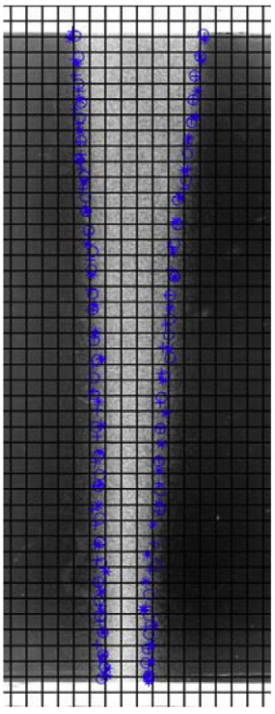

Fig. 2. Image of particle curtain captured by high speed camera. Size of the image is 17×45 cm.

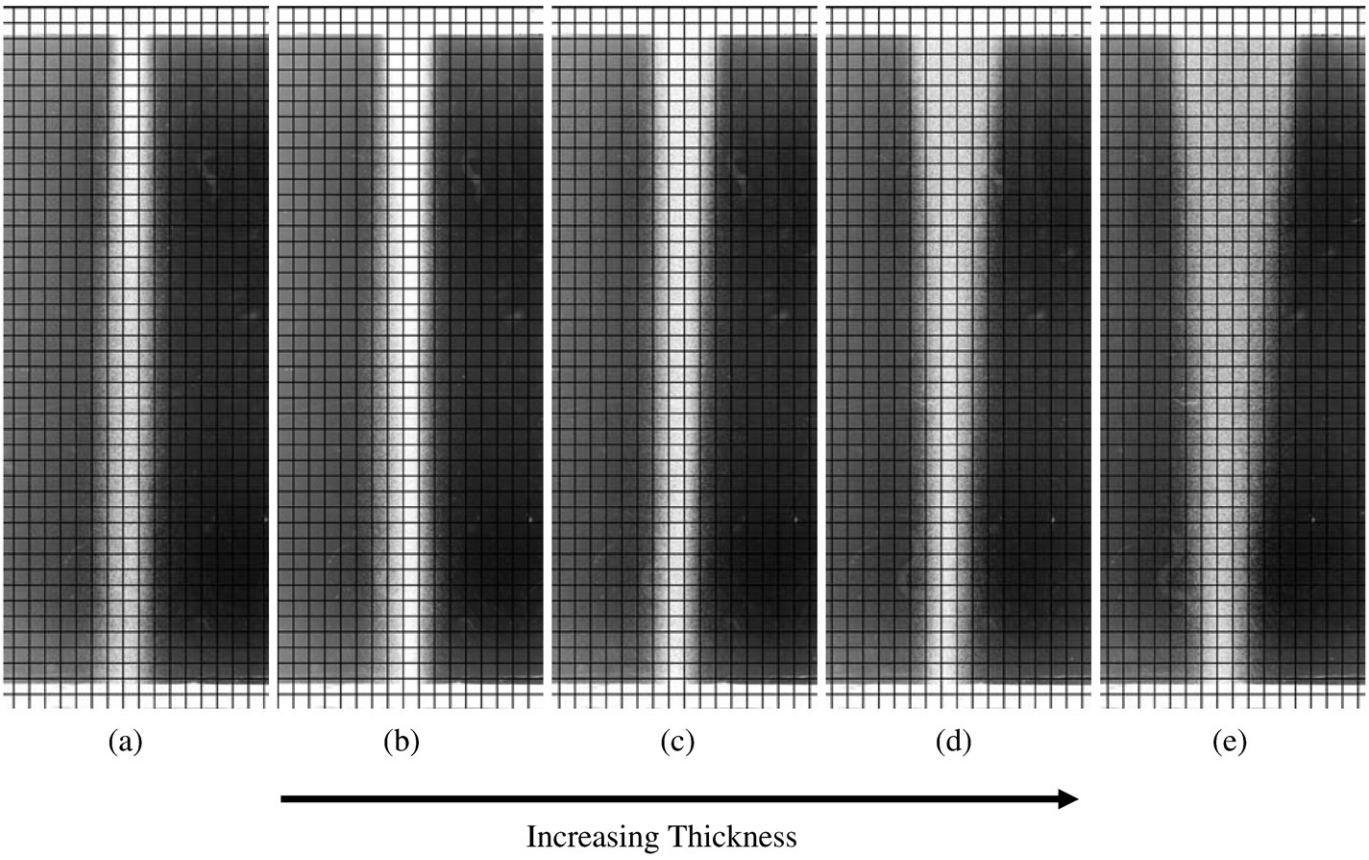

Fig. 3. Curtain structure with five different inlet thicknesses and relatively constant mass flow rates (0.040 kg/s) [(a) 2 cm, (b) 4 cm, (c) 6 cm, (d) 8 cm and (e) 10 cm].

The stagnant air was modelled as a continuous fluid phase and the falling solids as a dispersed phase with interparticle forces. The numerical domain was discretized with a 6 mm tetrahedral mesh, resulting in a total mesh of 137,969 nodes. The model was solved using CFX 5.7.1 until all residuals were less than 10^{-4} or 100 iterations had passed.

The three-dimensional flow behaviour of the gas and solid phases was solved using the Navier–Stokes equations combined with the industry standard $k-\varepsilon$ model [10] for turbulence in the continuous phase and a zero-equation model for the dispersed phase. A similar model has been successfully used to simulate the fluid dynamic behaviour of a curtain of particle falling through a horizontally-flowing gas stream Wardjiman et al. [17]). The governing equations are given below (the subscript α represents the current phase and β represents the other phase):

Continuity equation:

$$\frac{\partial}{\partial t}(r_\alpha \rho_\alpha) + \nabla \cdot (r_\alpha \rho_\alpha U_\alpha) = 0 \tag{1}$$

Momentum equation:

$$\frac{\partial (r_\alpha \rho_\alpha U_\alpha)}{\partial t} + \nabla \cdot (r_\alpha (\rho_\alpha U_\alpha \otimes U_\alpha)) = -r_\alpha \nabla P_\alpha + \nabla \cdot \left(r_\alpha \mu_\alpha \left(\nabla U_\alpha + (\nabla U_\alpha)^{T_\alpha} \right) \right) + r_\alpha \rho_\alpha g + g(\rho - \rho_{\text{ref}}) + B\left(U_\alpha - U_\beta\right) \tag{2}$$

where $B = \frac{3\mu_g r_p}{4d_p^2} Re \times C_D$ is used to describe the effects of drag forces on the gas. Re was calculated as $\frac{\rho_g U_g d_p}{\mu_g}$ and C_D was evaluated using the Schiller–Naumann equation [15]:

$$C_D = \frac{24}{Re}\left(1 + 0.15 Re^{0.687}\right). \tag{3}$$

In addition to the unsteady–state Navier–Stokes equations, the following equations were used to describe the effects of turbulence in the model.

Turbulent viscosity

$$\mu_{t\alpha} = 0.09 \rho_\alpha \frac{k_\alpha^2}{\varepsilon_\alpha} \tag{4}$$

Continuous phase turbulence model ($k-\varepsilon$ model)

Turbulent kinetic energy

$$\frac{\partial}{\partial t}\left(r_g \rho_g k_g\right) + \nabla \cdot \left(r_g \left(\rho_g U_g k_g - \left(\mu + \frac{\mu_{tg}}{\sigma_k} \right) \nabla k_g \right) \right) = r_g \left(P_{kg} - \rho_g \varepsilon_g \right) + T_{gp}^{(k)} \tag{5}$$

Turbulence dissipation rate

$$\frac{\partial}{\partial t}\left(r_g \rho_g \varepsilon_g\right) + \nabla \cdot \left(r_g \rho_g U_g \varepsilon_g - \left(\mu + \frac{\mu_{tg}}{\sigma_\varepsilon} \right) \nabla \varepsilon_g \right) = r_g \frac{\varepsilon_g}{k_g} \left(C_{\varepsilon 1} P_{kg} - C_{\varepsilon 2} \rho_g \varepsilon_g \right) + T_{gp}^{(k)} \tag{6}$$

where $C_{\varepsilon 1} = 1.44$, $C_{\varepsilon 2} = 1.92$, $\sigma_k = 1.0$ and $\sigma_\varepsilon = 1.3$ are constants [8]. The terms $T_{gp}^{(k)}$ and $T_{gp}^{(\varepsilon)}$ represent interphase transfer for k and ε respectively, however these are omitted in CFX 5.7.1 [1]).

Table 1
A summary of the experimental and calculation result for 5 different curtain thicknesses.

Curtain thickness (cm)	2	4	6	8	10
Initial particle vertical velocity (m/s)	1.85	1.64	1.56	1.44	1.42
Solid mass flow rate (kg/s)	0.041	0.042	0.041	0.039	0.040
Initial voidage	0.997	0.998	0.999	0.999	0.999

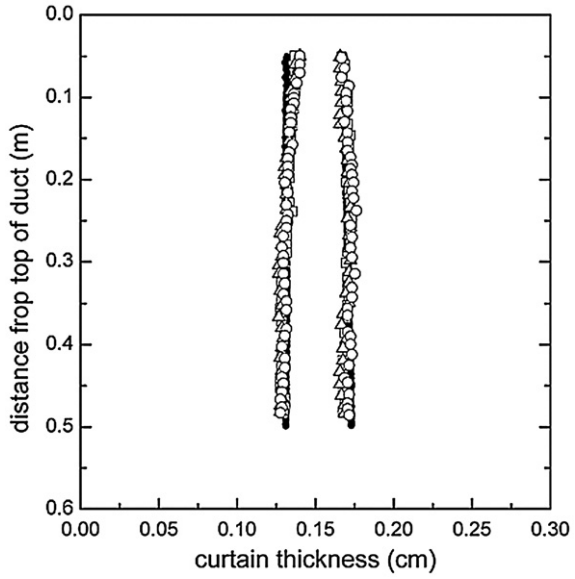

Fig. 4. Curtain structure with inlet thickness of 2 cm and mass flow rates of 0.040 kg/s (···· — CFD, ○ — run 1, □ — run 2, Δ — run 3).

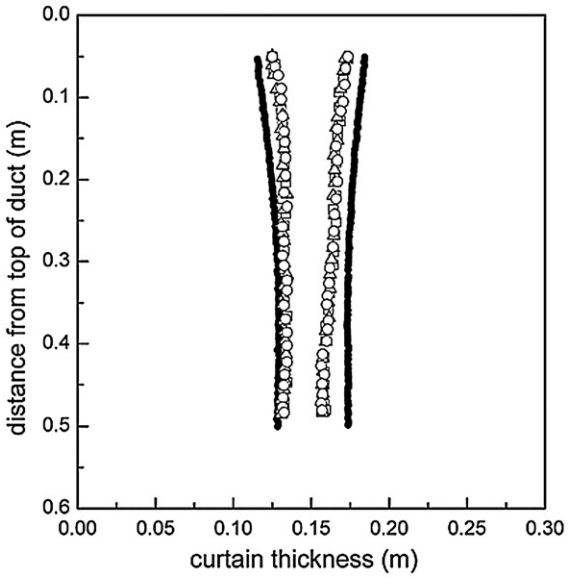

Fig. 6. Curtain structure with inlet thickness of 6 cm and mass flow rates of 0.040 kg/s (···· — CFD, ○ — run 1, □ — run 2, Δ — run 3).

Generation of turbulent energy

$$P_{kg} = \mu_{tg}\nabla U_g \cdot \left(\nabla U_g + \nabla U_g^T\right) - \frac{2}{3}\nabla . U_g\left(3\mu_{tg}\nabla . U_g + \rho_g k_g\right) + P_{kbg} \quad (7)$$

Buoyancy turbulence

$$P_{kbg} = -\frac{\mu_{tg}}{\rho_g} g \cdot \nabla \rho_g \quad (8)$$

Dispersed phase turbulence model (zero-equation model)

$$\mu_{ts} = \frac{\rho_s}{\rho_g}\mu_{tg}. \quad (9)$$

3.1. Boundary conditions

The inlet voidage of material was calculated based on experimental data using the following equation $r_{p0} = \frac{\dot{M}_p}{\rho_p U_{p0} A}$, where $\dot{M}_p$ is the mass flow rate of solids entering the system, U_{p0} is the initial velocity of the solids entering the duct, and A is the cross-sectional area of the solids inlet. In the absence of experimental data, the gas and solid inlets were given a turbulence intensity of 5% [2]. The remaining boundary conditions were modelled as walls governed by the no-slip condition.

3.2. Analysis of results

The results of the simulations were analysed using CFX 5.7.1 post-processor. The edges of the curtain were defined using a contour of constant voidage of 0.9994.

4. Results and discussion

Fig. 3 shows the experimentally determined curtain shapes for five different curtain inlet thicknesses, ranging from 2 cm to 10 cm. When the inlet particle curtain thickness was set at 2 cm, (Fig. 3(a)) the

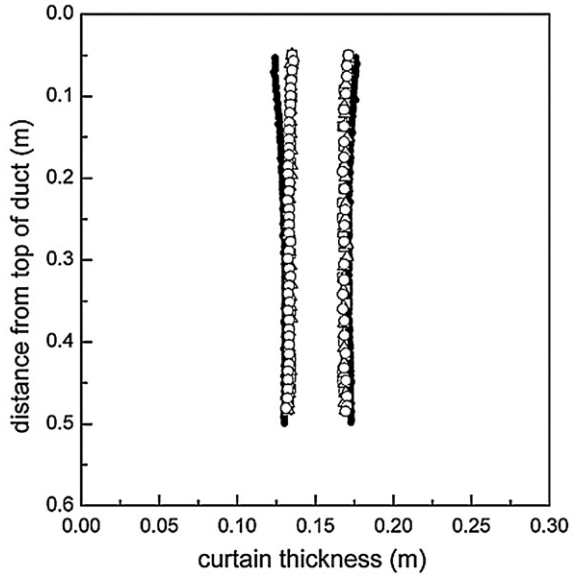

Fig. 5. Curtain structure with inlet thickness of 4 cm and mass flow rates of 0.040 kg/s (···· — CFD, ○ — run 1, □ — run 2, Δ — run 3).

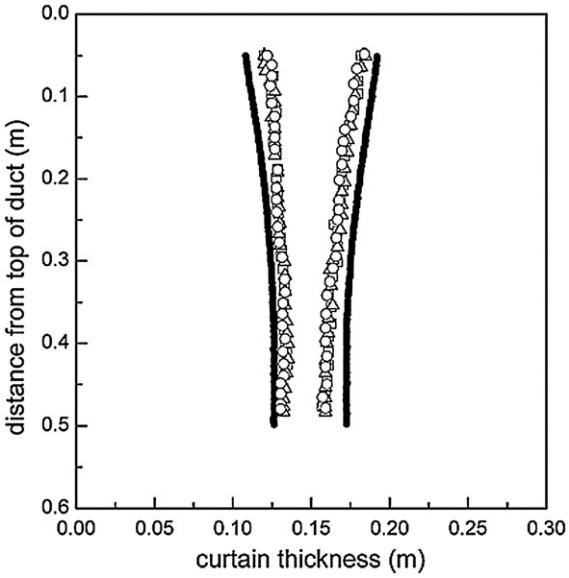

Fig. 7. Curtain structure with inlet thickness of 8 cm and mass flow rates of 0.040 kg/s (···· — CFD, ○ — run 1, □ — run 2, Δ — run 3).

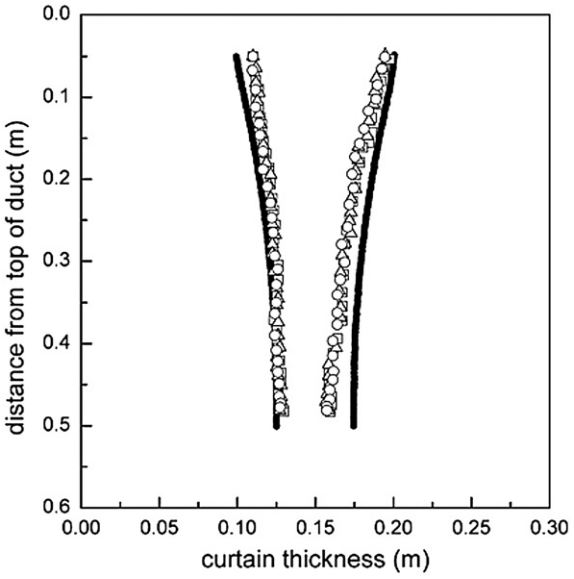

Fig. 8. Curtain structure with inlet thickness of 10 cm and mass flow rates of 0.040 kg/s (···· — CFD, ○ — run 1, □ — run 2, Δ — run 3).

particle curtain was found to diverge. When the inlet particle curtain thickness was set at 4 cm (Fig. 3(b)), the particle curtain showed a lower degree of divergence. When the inlet curtain thickness was increased to 6 cm, the curtain showed some convergence (Fig. 3(c)). Increasing convergence was observed as the inlet thickness was further increased to 8 cm and 10 cm (Fig. 3(d) and (e)). Measurement of the solids mass flow rates and the initial velocity of the particle curtain enabled calculation of the initial voidage of the curtains (see Table 1). We can therefore summarise the observations as follows. When a curtain with low initial voidage (inlet thickness of 2 cm) falls, a diverging curtain resulted. As the initial voidage of the particle stream increased (inlet thickness of 4 cm, 6 cm and 8 cm), the curtain became less divergent. Further increase in the initial voidage (inlet thickness of 10 cm) of the particle stream causes the curtain to become increasingly convergent.

Figs. 4–8 show the comparisons of experimentally determined curtain shapes with those predicted by the CFD model. As shown from these figures, the CFD model was able to predict the trends of the converging and diverging behaviour of the particle curtain.

A summary of the experimental and calculated results are given in Table 1.

5. Conclusion

An experimental study of the changing shape of a free-falling high-voidage particle curtain with changing inlet curtain thickness was presented. The images of the particle curtain shapes clearly showed that increasing the inlet curtain thickness from 2 cm to 10 cm caused the resultant particle curtain to become decreasingly divergent and then increasingly convergent. The shape of the particle curtain was tracked using high-speed video camera and compared with CFD simulations. The CFD model was able to predict the trends of converging and diverging behaviour of the particle curtain.

Nomenclature

C_D	drag coefficient
d	diameter, m
e	Particle–particle restitution coefficient
g	gravitational acceleration, m/s^2
g_0	Radial distribution function
k	turbulence kinetic energy per unit mass, m^2/s^2
P	pressure, Pa
P_s	Solids pressure
P_k	turbulence production due to viscous and buoyant forces, kg/m s^3
P_{kb}	turbulence production due to buoyant forces, kg/m s^3
l	Initial curtain thickness
r	volume fraction, m^3/m^3
Re	Reynolds number $\left(\frac{\rho_g(\dot{y}_p - \dot{y}_g)d_p}{\mu_g}\right)$
T	Temperature, K
$T_{gp}^{(k)}$	interphase turbulent kinetic energy transfer term
$T_{gp}^{(\varepsilon)}$	interphase turbulence dissipation transfer term
w	Curtain width
ε	turbulence dissipation rate, m^2/s^3
Θ_S	Granular temperature
μ	dynamic viscosity, kg/m s
μ_t	turbulent dynamic viscosity, kg/m s
ρ	density, kg/m^3
ρ_{ref}	reference gas density calculated at the centre of the duct outlet, kg/m^3

Subscripts

s	particle
g	gas

References

[1] CFX Solver Theory Guide, Ansys Europe, Ltd., 2006.
[2] CFX Solver Modelling Guide, Ansys Europe, Ltd., 2006.
[3] S. Cooper, C.J. Coronella, CFD simulations of particle mixing in a binary fluidized bed, Powder Technology 151 (2005) 27–36.
[4] R.C. Darton, The structure and dispersion of jets of solid particles falling from a hopper, Powder Technology v13 (1976) 241–250.
[5] W. Du, X. Bao, J. Xu, W. Wei, Computational Fluid Dynamics (CFD) modelling of spouted bed: assessment of drag coefficient correlations, Chemical Engineering Science 61 (2006) 1401–1420.
[6] M. Hidayat, R. Rasmuson, Some aspects on gas–solid flow in a u-bend: numerical investigation, Powder Technology 153 (2005) 1–12.
[7] W.D.L. Hemeon, Air Flow in Materials Handling System, Plant and Process Ventilation, Industrial Press, New York, 1963, pp. 120–159.
[8] B.E. Launder, D.B. Spaulding, Lectures in Mathematical Models of Turbulence, Academic Press, 1972.
[9] H. Nakamura, S. Watano, Numerical modelling of particle fluidization behaviour in a rotating fluidized bed, Power Technology 171 (2007) 106–117.
[10] T. Norton, D.W. Sun, Computational Fluid Dynamics (CFD) — an effective and efficient design and analysis tool for the food industry: a review, Trends in Food Science and Technology 17 (2006) 600–620.
[11] K. Ogata, F. Funatsu, Y. Tomita, Experimental investigation of a free falling powder jet and the air entrainment, Powder Techmology v115 (2001) 90–95.
[12] M.A.E. Plinke, D. Leith, D.B. Holstein, M.G. Boundy, Experimental examination of factors than affect dust generation, American Industrial Hygiene Association Journal v52 (1991) 521–528.
[13] R.T. Pring, J.F. Knudsen, R. Dennis, Design of exhaust ventilation for solid materials handling, Industrial and Engineering Chemistry v41 (n11) (1949) 2442–2450.
[14] P.H. Rothe, J.A. Block, Aerodynamic behaviour of liquid spray, International Journal of Multiphase Flow v3 (1977) 263–272.
[15] L. Schiller, A. Naumann, Über die grundlegenden berechungen bei der schwerkraftaufbereitung, Ver. deut. Ing., vol. 77, 1933, pp. 318–320.
[16] T. Uchiyama, Numerical analysis of particulate jet generated by free falling particles, Powder Technology v145 (2004) 123–130.
[17] C. Wardjiman, A. Lee, M. Sheehan, M. Rhodes, Behaviour of a curtain of particles falling through a horizontally-flowing gas stream, Powder Technology v188 (2) (2008) 110–118.
[18] P. Wypych, D. Cook, P. Cooper, Controlling dust emissions and explosion hazards in powder handling plants, Chemical Engineering and Processing v44 (2005) 323–326.